Inhibition of *Jiawei Foshou San* on invasion and metastasis through MMP/TIMP signaling in endometriosis

Ying Zhang
Southwest University
Jiahui Wei
Southwest University
Yi Tan
Southwest University
Chengling Zhang
Southwest University
Pingli Xu
Chongqing City Hospital of Traditional Chinese Medicine
Yi Chen (rachelcy@swu.edu.cn)
Southwest University

Research

Keywords: Jiawei Foshou San, Endometrial cells, Xenograft endometriosis, Invasion and metastasis, MMP/TIMP signaling

Posted Date: May 22nd, 2020

DOI: https://doi.org/10.21203/rs.3.rs-29684/v1

Abstract

Background: The new formula Jiawei Foshou San (JFS) is consisted of ligustrazine, ferulic acid and tetrahydropalmatine designed from Foshou San . Previously JFS inhibited the growth of rat autograft endometriosis with unclear mechanism. To uncover the effect of JFS on invasion and metastasis in endometrial cells and xenograft endometriosis.

Methods: In vitro , cell viability assay was performed for IC50 measurement in hEM15A and HEC1-B cells after treating JFS. Effects of JFS on invasion and metastasis were analyzed in scratch wound and transwell assay. In vivo , effect of JFS was evaluated in xenogeneic transplantation of endometriosis model. The gene and protein expression of MMP/TIMP signaling were inspected in vitro and in vivo .

Results: Inhibitory effects of JFS were investigated with dose-dependent manner in hEM15A and HEC1-B cells. JFS significantly inhibited the invasion and metastasis in dose- and time-dependent manner. In xenograft endometriosis, JFS reduced the volume of ectopic endometrium. In-depth study, inactive MMP/TIMP signaling expressed the lower MMP-2/9, higher TIMP-1 by JFS in vitro and in vivo .

Conclusions: JFS prevent invasion and metastasis via inactivation of MMP/TIMP signaling in endometrial cells and xenograft endometriosis. It reveals the potential mechanism of JFS on endometriosis and the benefit for further application.

Background

Endometriosis (EMS) is a disease caused by the active endometrial cells growing outside the endometrium. Although the unclear pathogenesis of EMS, the known menstrual reflux hypothesis regards that implantation of viable endometrial cells is the essential process in the menstrual effluent of menstruation. This pathological step mainly contains invasion and metastasis [1, 2]. The imbalance between matrix metalloproteinases (MMPs) and tissue inhibitors of MMPs (TIMPs) are the vital mechanism of invasion and metastasis. MMP-2 and MMP-9 promote the invasion and metastasis through degradation of extracellular matrix. On the contrary, TIMP-1 has the antagonistic effects on MMPs [3].

EMS belongs to blood stasis syndromes with treatment of activating blood and dissolving stasis in traditional Chinese medicine [4, 5]. Famous gynecological prescription Foshou san is performed in blood stasis syndromes, including endomtriosis [6]. JFS, a new Chinese compound, is designed from Foshou san, which is composed of ferulic acid, ligustrazine and tetrahydropalmatine. In previous studies, the potential therapeutic effect of JFS have been detected in rat autograft EMS model [5, 7, 8], but with unclear effect on endometrial cells and xenograft EMS model.

In this paper, IC50 of JFS on hEM15A and HEC1-B endometrial cells were measured *in vitro*. Then the anti-metastasis of JFS were detected by scratch wound and transwell assays. Therapeutic effect of JFS on

xenograft EMS was observed *in vivo*. The regulations of MMP/TIMP signaling were investigated by JFS *in vitro* and *in vivo*.

Methods

Animals and chemicals

Female C3H mice weighing 18-20 g were purchased from Beijing Vital River Laboratory Animal Technology Co., Ltd. (Certification no. SCXK [Jing]2016-0006) (Beijing, China). Female nude mice weighing 18-20 g were purchased from Hunan Silaike Jingda Laboratory Animal Co., Ltd. (Certification no. SCXK [Xiang]2016-0002) (Hunan, China). The mice were sheltered in the Experimental Center, Southwest University. This study was executed in rigorous accordance with the recommendations in the Guidelines for the Care and Use of Laboratory Animals of Southwest University (Approval no. 0002183). To minimize suffering, anaesthesia and other necessary efforts were performed.

Ferulic acid, ligustrazine hydrochloride and tetrahydropalmatine were purchased from Nanjing Zelang Medical Technology Co., Ltd (Nanjing, China), with the purity of 99.8, 99.3, 98.1% respectively. In vitro, they were dissolved in DMSO at the ratio of 1:0.5:0.3 for cells treatment. In vivo, three monomers were dematerialized with the same ratio in 0.5% CMC-Na for mice usage. Gestrinone was provided by Zizhu Pharmaceutical Co., Ltd. Beijing, China).

Cell culture

The human endometriosis-derived eutopic endometrium stromal cells hEM15A presented by Professor Xiaohong Chang of Peking University People's Hospital (Beijing, China). The endometrial adenocarcinoma cells HEC1-B were purchased from the Chinese Centre for Type Cultures Collections (CCTCC, Wuhan, China). hEM15A cells were cultured in DMEM/F12 (Gibco, Grand Island, NY, USA) with 20% FBS (Hyclone, Shanghai, China). HEC1-B cells were cultured in MEM medium (Gibco, Grand Island, NY, USA) with 10% FBS (Natocor, Argentina). Both of them were put into humidified incubator at 37°C with 5% CO_2.

Cell viability assay

hEM15A and HEC1-B cells were seeded at 6-8×10^3, 8-10×10^3 cells/well in 96-well plates respectively. hEM15A cells were treated with JFS (0, 156, 313, 625, 1250 and 2500 μg.ml^{-1}), and HEC1-B cells were cultured with JFS (0, 15, 46, 139, 417 and 1250 μg.ml^{-1}) for 24 or 48 h. After treatment, the cells were incubated with MTT solution for 4 hours. Dissolved in DMSO, endometrial cells were measured in a microplate reader. IC50 values were calculated by GraphPad Prism5 Software (5.01 version, La Jolla, CA, USA).

Scratch wound assay

hEM15A and HEC1-B cells were put in a 24-well plate at a density of 6-8×10^4, 8-10×10^4 cells/well respectively. When the cell confluence reached approximately 80%, wounded traces were produced by 1 ml pipette tip vertically in the well plate. Added medium with JFS, endometrial cells were observed and photographed under 50´ magnification at 0, 12, 24 and 48 h. The area of the scratched area was calculated using Image pro plus 6.0 software (Media Cybernetics, Silver Spring, USA). Scratch closure rate = (average scratch area at 0 h - average scratch area at each time point) / average scratch area at 0 h) × 100%.

Transwell assay

The transwell inserts without matrigel (Corning, New York, USA) were put into a 24-well plate. 3×10^4 hEM15A or HEC1-B cells/well were placed into upper chamber with serum-free JFS medium. 5% FBS medium without JFS were added to the lower chamber. After incubation at 37℃ for 12, 24 and 48 hours, non-migrating cells on the surface of upper chamber were swiped by a cotton swab. The migrated cells in bottom were fixed with Paraformaldehyde, and then stained with crystal violet. The migratory cell numbers were counted in 5 random fields at 100×magnification.

Xenograft EMS model and treatment

As attested by the previous study [9, 10], bilateral uterus of estrus C3H mice were cut into 4 mm^2 tissue blocks and transplanted into the subcutaneous abdomen of 71 nude mice. After operation, nude mice were administrated with 2 $mg{\cdot}kg^{-1}$ estradiol benzoate by intramuscular injection once every 5 days. Volume of endometrial allografts was calculated by vernier caliper after 28 days with a formula (0.52×length×width×height). Endometrial allograft explants, larger than 4.5 mm^3 with surface blood, were regarded as the successful EMS models in the second laparotomy. Then 4 groups were randomly established with EMS mice, including were EMS group with 0.5% CMC-Na, 90, 180, 360 $mg{\cdot}kg^{-1}$ Neiyixiao groups, and 0.05 $mg{\cdot}kg^{-1}$ gestrinone group. Another 6 female C3H mice without transplantation were administered 0.5% CMC-Na as control group. After administration for 28 days by gavage, the volumes of the ectopic tissues were measured again.

RNA isolation and qPCR

Total RNA was extracted using the TRIzol reagent (Invitrogen, CA, USA) and then reversely transcribed into cDNA using the PrimeScript™ RT Reagent Kit (Takara, China). Real-time PCR was conducted in CFX96 Real-Time System (Bio-Rad, USA) and fluorescent quantification was detected with SYBR™ Green Master Mix (Thermo Fisher Scientific, USA). The relative mRNA expression was calculated by the $2^{-\Delta\Delta CT}$ method using primer sequences (Table 1), which were synthesized by Dingguo Changsheng Biotechnology (Beijing, China). GAPDH gene as the control reference.

Table 1 primer sequences of RT-qPCR

Species	Primer name	Sequences (5'-3')
Mouse	MMP-2-F	CCCTCAAGAAGATGCAGAAGTTC
	MMP-2-R	ATCTTGGCTTCCGCATGGT
	MMP-9-F	ACCAAGGGTACAGCCTGTTCCT
	MMP-9-R	GGTAGCTATACAGCGGGTACATGA
	TIMP-1-F	CTTGGTTCCCTGGCGTACTC
	TIMP-1-R	ACCTGATCCGTCCACAAACAG
	GAPDH-F	CCTGGAGAAACCTGCCAAGTAT
	GAPDH-R	GGTCCTCAGTGTAGCCCAAGAT
Human	MMP-2-F	GGCCCTGTCACTCCTGAGAT
	MMP-2-R	GGCATCCAGGTTATCGGGGA
	MMP-9-F	TGGACGATGCCTGCAACGTG
	MMP-9-R	GTCGTGCGTGTCCAAAGGCA
	TIMP-1-F	CAATTCCGACCTCGTCATCAG
	TIMP-1-R	CTTGGAACCCTTTATACATCTTGG
	GAPDH-F	AATGGGCAGCCGTTAGGAAA
	GAPDH-R	GCCCAATACGACCAAATCAGAG

Western blot analysis

Total Proteins were extracted form tissues and cells by RIPA protein lysis buffer with protease inhibitors on ice. Equal amounts of protein were separated by SDS-PAGE and transferred onto poplvinylidene fluoride membrane (Millipore, USA). The membranes were incubated overnight at 4°C with primary rabbit anti-MMP-2 and rabbit anti-MMP-9 (1:100 dilution; Boster Biological Technology, Wuhan, China), rabbit anti-TIMP-1 (1:300 dilution; Proteintech Biotechnology, Wuhan, China), rabbit anti-β-actin (1:5000 dilution; Proteintech Biotechnology, Wuhan, China). After washing with TBST, membranes were incubated with HRP-labeled goat anti-rabbit secondary antibody (1:1000 dilution; Multi Sciences, Hangzhou, China). Chemiluminescent signals were captured analyzed with the Tanon 5200 imaging system (Tanon, China). β-actin was used as an internal control.

Statistical analysis

All data were presented as the mean ± SD and likened by one-way ANOVA test applying SPSS 21.0 software. $P<0.05$ was considered statistically significant.

Results

IC50 of JFS on endometrial cells

To reveal the IC50 of JFS on hEM15A and HEC1-B cells, these two cells viability were measured by MTT method after treated with different concentrations of *JFS* respectively for 24 or 48 h. In hEM15A cells, IC50 of JFS were 839.30±121.11 or 483.53 ±156.91 μg.ml^{-1} for 24 or 48 h respectively (Fig. 1A). In HEC1-B cells, the IC50 values were 625.20±59.52 or 250.30±68.12 μg.ml^{-1} for 24 or 48 h JFS treatment respectively (Fig 1 B). Moreover, significant inhibitory effects of JFS were investigated with dose-dependent manner in hEM15A and HEC1-B cells. It was also notable that IC50 of JFS on HEC1-B cells were obviously lower than that on hEM15A cells. It was indicated that HEC1-B cells might be more sensitive to JFS.

Constraint of endometrial cell migration and invasion by JFS

Scratch wound assay is commonly used to detect the cell migration. IC50 concentration of JFS was performed as middle dose. The low or high dose was half or double of IC50 concentration. The endometrial cells were observed for 12 and 24h with IC50 24h JFS, or for 24 and 48h with IC50 48h JFS. After treated with JFS for 12 and 24h, wound closure of JFS were obviously decreased compared with control in hEM15A and HEC1-B cells (P<0.01) (Fig. 2A-D). Meanwhile, JFS significantly resisted the spread of both cell lines along the edge of wound scratch, with no effect of 240 μg.ml^{-1} JFS in hEM15A cells (Fig. 2E-H). This indicated that JFS markedly inhibited cell migration with dose- and time-dependent manner in scratch wound assay.

Transwell assay was performed to measure the effects of JFS on cell migration and invasion. Maintain identical time and concentration of JFS were applied as previous scratch wound experiment. Results showed that JFS significantly reduced the number of migratory cells passing through the chamber membrane vs control group in hEM15A (Fig. 3A, C, E, G) and HEC1-B cells (Fig. 3B, D, F, H). This suggested that JFS obviously suppressed cell migration and invasion with dose- and time-dependent manner in transwell assay.

Regulation of JFS on MMP/TIMP signaling in vitro

After treated with JFS for 24 h, the mRNA level of MMP-2 and MMP-9 obviously attenuated compared to control group, while TIMP-1 expanded especially in 960 μg.ml^{-1} JFS group of hEM15A cell (P<0.05) (Fig. 4A-C). Moreover, the mRNA level of MMP-2 and MMP-9 were significantly downregulated and TIMP-1 was upregulated in 1250 μg.ml^{-1} JFS group of HEC1-B cell (P<0.05) (Fig. 4D-F).

Furthermore, the protein expression was consistent with gene expression of MMP/TIMP signaling. The protein level of MMP-2 and MMP-9 decreased in 240, 480 and 960 μg.ml^{-1} JFS groups, accompanied with accumulation of TIMP-1 compared with the control group in hEM15A cells (P<0.01) (Fig. 5A-D). At the same time, the protein level of MMP-2 in 1250 μg.ml^{-1} group, and MMP-9 in 625 μg.ml^{-1} group were

significantly downregulated, though TIMP-1 were upregulated in 625 and 1250 μg.ml^{-1} JFS groups compared with control group in HEC1-B cells (P<0.05) (Fig. 5E-H).

Inhibition of ectopic endometrium volume using JFS

28 days after transplantation, 56 of 71 nude mice were found xenograft EMS in the second laparotomy. The successful rate of model was 79%. There was no remarkable difference in the volume of the ectopic endometrium between all groups before administration. After treatment for 28 days, the volume of ectopic issue was detected in different groups and compared with pretreatment. In the EMS group, the volume of ectopic endometrium had no difference between posttreatment with pretreatment. There were significantly depression observed in 90, 180 and 360 mg·kg^{-1} JFS groups, respectively (P<0.05). The volume of ectopic endometrium tissue was minimized in gestrinone group (P<0.05) (Fig. 6A). This suggests that JFS restrained the growth of transplant in a dose-independent manner.

Adjustment of MMP/TIMP signaling by JFS in vivo

After treatment with JFS, genes and proteins of MMP-2, MMP-9, and TIMP-1 were detected in ectopic endometrial tissues. As evidenced by qRT-PCR, the mRNA level of MMP-2 and MMP-9 were significantly higher while TIMP-1 was lower in EMS group than those in control group (P<0.01). The mRNA level of MMP-2 and MMP-9 were obviously downregulated and TIMP-1 was upregulated in JFS groups than those in EMS group (P<0.05) (Fig. 6B-D). The protein levels of MMP-2 and MMP-9 were remarkably raised with reducing TIMP-1 in EMS group compared with control group (P<0.05). JFS obviously decreased the protein level of MMP-2 and MMP-9, and increased the protein level of TIMP-1 (P<0.05) (Fig. 6E-H).

Discussion

JFS has been proved to display the potential anti-endometriosis effects in rat autograft EMS model [5, 7, 8]. The underlying mechanism of JFS embrace diminishing the growth of EMS, suppression of E2, inflammation and epithelial mesenchymal transformation. Therefore, we detected the effects of JFS on endometrial cells and xenograft EMS model. In this study, JFS markedly inhibited invasion and metastasis both *in vitro* and *in vivo*. It related to the decrease of MMP-2, MMP-9, and increase of TIMP-1.

In cell viability assay, IC50 of JFS were different in hEM15A and HEC1-B cells, which were human endometriosis-derived eutopic endometrium stromal cells and endometrial adenocarcinoma cells. It was also notable that IC50 in HEC1-B cells were obviously lower than that in hEM15A cells. It was indicated that HEC1-B cells might be more sensitive to JFS. There are no researches of JFS or JFS ingredients, ferulic acid, ligustrazine, or tetrahydropalmatine on endometrial cancer, except *Angelica sinensis* showed weak binding with ER in endometrial cancer cells [11]. Therefore, our results are suggested that JFS or JFS ingredients might have the potential effects on endometrial cancer. It needs further research.

In traditional Chinese medicine, blood stasis syndromes should be treated with Huoxue Huayu recipes to activate blood and dissolve stasis [12, 13]. Whether activating blood and dissolving stasis mean inhibit

invasion and metastasis or not will depend on individual situations. On one hand, the suppression of metastatic potential is found in ligustrazine, ferulic acid, or tetrahydropalmatine in various kinds of cancer, for example osteosarcoma, fibrosacroma, and breast cancer [14-16]. Especially, ligustrazine shows downregulation of MMP-2/9, and upregulation of TIMP-1. In neuropathic pain or blood-brain barrier injury, ligustrazine or tetrahydropalmatine decreases the expression of MMP-2/9 [17, 18]. On the other hand, using ligustrazine, bone marrow mesenchymal stem cells are promoted to migrate by raising MMP-2/9 [19]. In our experiment, JFS inhibited the growth of endometrial cells and ectopic endometrium in xenograft EMS model. Invasion and metastasis were restrained by JFS, thrgouth suppressing MMP-2/9 and accumulating TIMP-1 *in vivo* and *in vitro*. Considering the conflicting reports, it is worthwhile to explore role of JFS on different blood stasis syndrome diseases.

Conclusion

JFS prevented cell variability, invasion and metastasis in endometrial hEM15A and HEC1-B cells, meanwhile reduced volume of ectopic endometrium in xenograft EMS. It is related to the regulation of MMP/TIMP signaling by JFS, through attenuating MMP-2 and MMP-9, accumulating TIMP-1 both *in vitro* and *in vivo*. These results supply the pharmacological prove for JFS evaluation and application.

Abbreviations

JFS, Jiawei Foshou San; EMS, Endometriosis; GTN, gestrinone; MMPs, matrix metalloproteinases; TIMPs, tissue inhibitors of MMPs.

Declarations

Authors' contributions

YZ and JW performed the major research in equal contribution. YT, CZ, and PX provided the technical support. PX contributed to final approval of the version to be published. YC designed the study and revised the manuscript.

Acknowledgements

Not applicable.

Funding

This work was supported by grants from National Natural Science Foundation of China (No. 81773984, No. 81402441), Southwest University Undergraduate Science and Technology Innovation Fund (No.20162902003), and SWU National Experimental Demonstration Center of Pharmacy (No. XY2017-CXZD-04, YX2017-CXYB-01).

Availability of data and materials

The datasets in this study are available from the corresponding author on reasonable request.

Ethics approval and consent to participate

The animal care and experimental procedures in this study were approved by the Institutional Animal Care and Use Committee of Southwest University.

Consent for publication

Not applicable.

Competing interests

The authors declare that they have no competing interests.

References

[1] A. Mihailovici, M. Rottenstreich, S. Kovel, I. Wassermann, N. Smorgick, Z. Vaknin, Endometriosis-associated malignant transformation in abdominal surgical scar: A PRISMA-compliant systematic review, Medicine (Baltimore) 96(49) (2017) e9136.

[2] M.H. Chui, T.L. Wang, I.M. Shih, Endometriosis: benign, malignant, or something in between?, Oncotarget 8(45) (2017) 78263-78264.

[3] L. Herszenyi, I. Hritz, G. Lakatos, M.Z. Varga, Z. Tulassay, The Behavior of Matrix Metalloproteinases and Their Inhibitors in Colorectal Cancer, Int J Mol Sci 13(10) (2012) 13240-13263.

[4] F. Liao, Herbs of activating blood circulation to remove blood stasis, Clin Hemorheol Microcirc 23(2-4) (2000) 127-31.

[5] Y. Chen, J. Wei, Y. Zhang, W. Sun, Z. Li, Q. Wang, X. Xu, C. Li, P. Li, Anti-endometriosis Mechanism of Jiawei Foshou San Based on Network Pharmacology, Front Pharmacol 9 (2018) 811.

[6] H. Bai, P.Q. Li, J. Liu, X.P. Liu, [Association analysis on traditional efficacy and modern research of Foshou San], Chinese Traditional Patent Medicine 36(3) (2014) 601-604.

[7] J.H. Wei, B.X. Zhao, C.L. Zhang, B.B. Shen, Y. Zhang, C.X. Li, Y. Chen, Jiawei Foshou San Induces Apoptosis in Ectopic Endometrium Based on Systems Pharmacology, Molecular Docking, and Experimental Evidence, Evid-Based Compl Alt 2019 (2019).

[8] Q. Tang, F.H. Shang, X.C. Wang, Y. Yang, G. Chen, Y. Chen, J.F. Zhang, X.Y. Xu, Combination use of ferulic acid, ligustrazine and tetrahydropalmatine inhibits the growth of ectopic endometrial tissue: A multi-target therapy for endometriosis rats, Journal of Ethnopharmacology 151(3) (2014) 1218-1225.

[9] J.A. Attaman, A.K. Stanic, M. Kim, M.P. Lynch, B.R. Rueda, A.K. Styer, The anti-inflammatory impact of omega-3 polyunsaturated Fatty acids during the establishment of endometriosis-like lesions, Am J Reprod Immunol 72(4) (2014) 392-402.

[10] C.W. Cheng, D. Licence, E. Cook, F. Luo, M.J. Arends, S.K. Smith, C.G. Print, D.S. Charnock-Jones, Activation of mutated K-ras in donor endometrial epithelium and stroma promotes lesion growth in an intact immunocompetent murine model of endometriosis, J Pathol 224(2) (2011) 261-9.

[11] J.H. Liu, J.E. Burdette, H.Y. Xu, C.G. Gu, R.B. van Breemen, K.P.L. Bhat, N. Booth, A.I. Constantinou, J.M. Pezzuto, H.H.S. Fong, N.R. Farnsworth, J.L. Bolton, Evaluation of estrogenic activity of plant extracts for the potential treatment of menopausal symptoms, J Agr Food Chem 49(5) (2001) 2472-2479.

[12] P.P. Huang, S.G. Wang, G.X. Hua, [Observation on blood flow changes in 34 cases of progressive systemic scleroderma treated with Chinese herbal medicine], Zhongguo Zhong Xi Yi Jie He Za Zhi 14(2) (1994) 86-8, 68.

[13] X.-f.F. Yin-quan Deng, Jian-ping Li, Relationship Between Phlegm-Stasis Syndrome and Fibrinolytic Status in Patients With Non-Alcoholic Fatty Liver, Zhongguo Zhong Xi Yi Jie He Za Zhi 25(1) (2005) 22-4.

[14] S. Yodkeeree, P. Wongsirisin, W. Pompimon, P. Limtrakul, Anti-invasion effect of crebanine and O-methylbulbocapnine from Stephania venosa via down-regulated matrix metalloproteinases and urokinase plasminogen activator, Chem Pharm Bull (Tokyo) 61(11) (2013) 1156-65.

[15] X. Zhang, D. Lin, R. Jiang, H. Li, J. Wan, H. Li, Ferulic acid exerts antitumor activity and inhibits metastasis in breast cancer cells by regulating epithelial to mesenchymal transition, Oncol Rep 36(1) (2016) 271-8.

[16] M. Fang, X. Mei, H. Yao, T. Zhang, T. Zhang, N. Lu, Y. Liu, W. Xu, C. Wan, beta-elemene enhances anticancer and anti-metastatic effects of osteosarcoma of ligustrazine in vitro and in vivo, Oncol Lett 15(3) (2018) 3957-3964.

[17] L. Jiang, C.L. Pan, C.Y. Wang, B.Q. Liu, Y. Han, L. Hu, L. Liu, Y. Yang, J.W. Qu, W.T. Liu, Selective suppression of the JNK-MMP2/9 signal pathway by tetramethylpyrazine attenuates neuropathic pain in rats, J Neuroinflammation 14(1) (2017) 174.

[18] X.W. Mao, C.S. Pan, P. Huang, Y.Y. Liu, C.S. Wang, L. Yan, B.H. Hu, X. Chang, K. He, H.N. Mu, Q. Li, K. Sun, J.Y. Fan, J.Y. Han, Levo-tetrahydropalmatine attenuates mouse blood-brain barrier injury induced by focal cerebral ischemia and reperfusion: Involvement of Src kinase, Sci Rep 5 (2015) 11155.

[19] J. Wang, T.B. Qu, L.S. Chu, L. Li, C.C. Ren, S.Q. Sun, Y. Fang, [Ligustrazine Promoted the Migration of Bone Marrow Mesenchymal Stem Cells by Up-regulating MMP-2 and MMP-9 Expressions], Zhongguo Zhong Xi Yi Jie He Za Zhi 36(6) (2016) 718-23.

Figures

Figure 1

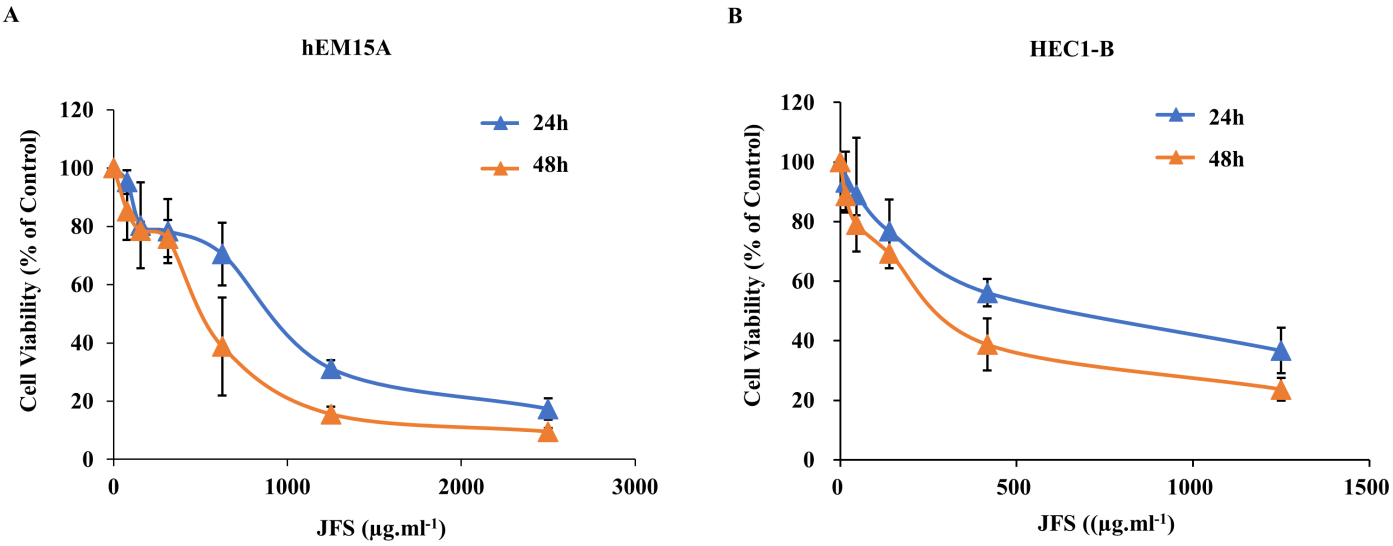

Figure 1

JFS inhibited endometrial cells viability. hEM15A (A) and HEC1-B (B) cells were treated with various concentrations of JFS for 24 and 48 h, and then analyzed by MTT assay. JFS, Jiawei Foshou San.

Figure 2

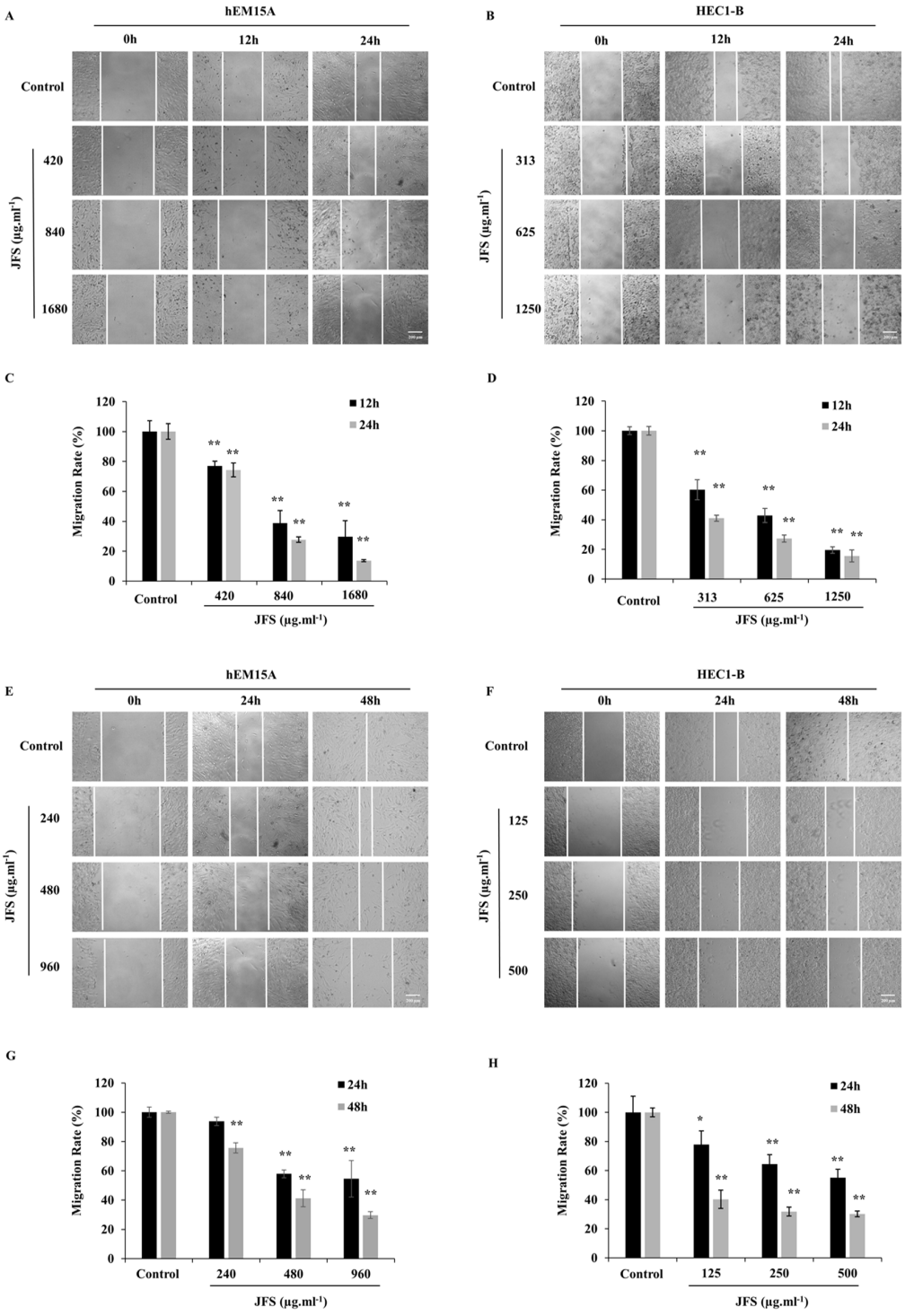

Figure 2

Migratory effects of JFS on endometrial cells. hEM15A (A, C) and HEC1-B (B, D) cells were scratched by a sterile pipette tip and treated with IC50 24h JFS for 12 and 24 h. hEM15A (E, G) and HEC1-B (F, H) cells were scratched by a sterile pipette tip and treated with IC50 48h JFS for 24 and 48 h. Photomicrographs showed representative wound scratches at different time points after wounding. *P<0.05 to control group, **P<0.01 to control group. Columns, mean (n=3). Bars, SD. Scale bar=200 μm. JFS, Jiawei Foshou San.

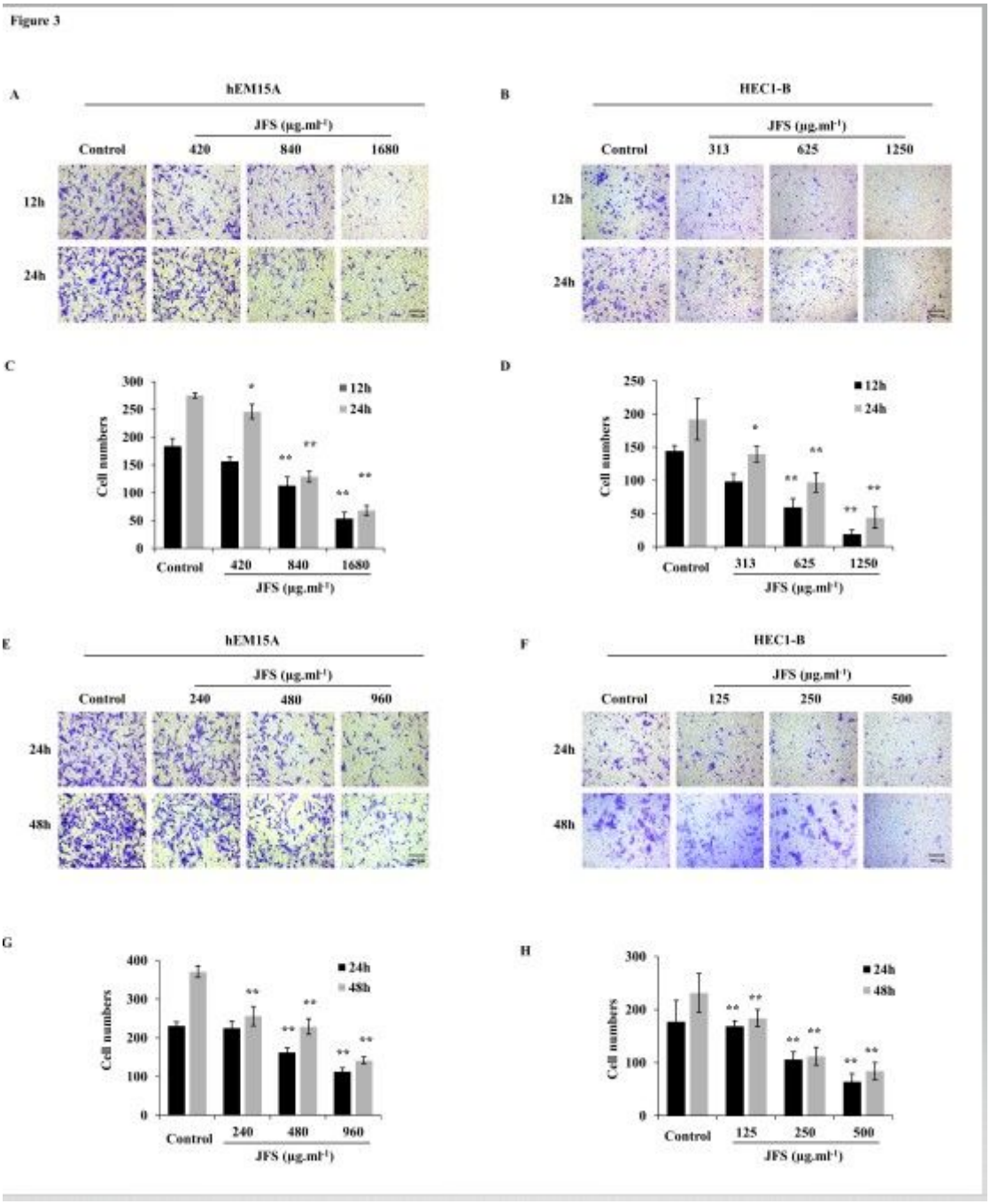

Figure 3

JFS restrained migration and invasion of endometrial cells. hEM15A (A, C) and HEC1-B (B, D) cells were performed in transwell assay and treated with IC50 24h JFS for 12 and 24 h. hEM15A (E, G) and HEC1-B (F, H) cells were performed in transwell assay treated with IC50 48h JFS for 24 and 48 h. The number of migrated cells was quantified in five random fields from three independent experiments. *P<0.05 to control group, **P<0.01 to control group. Columns, mean (n=3). Bars, SD. Scale bar=500 μm. JFS, Jiawei Foshou San.

Figure 4

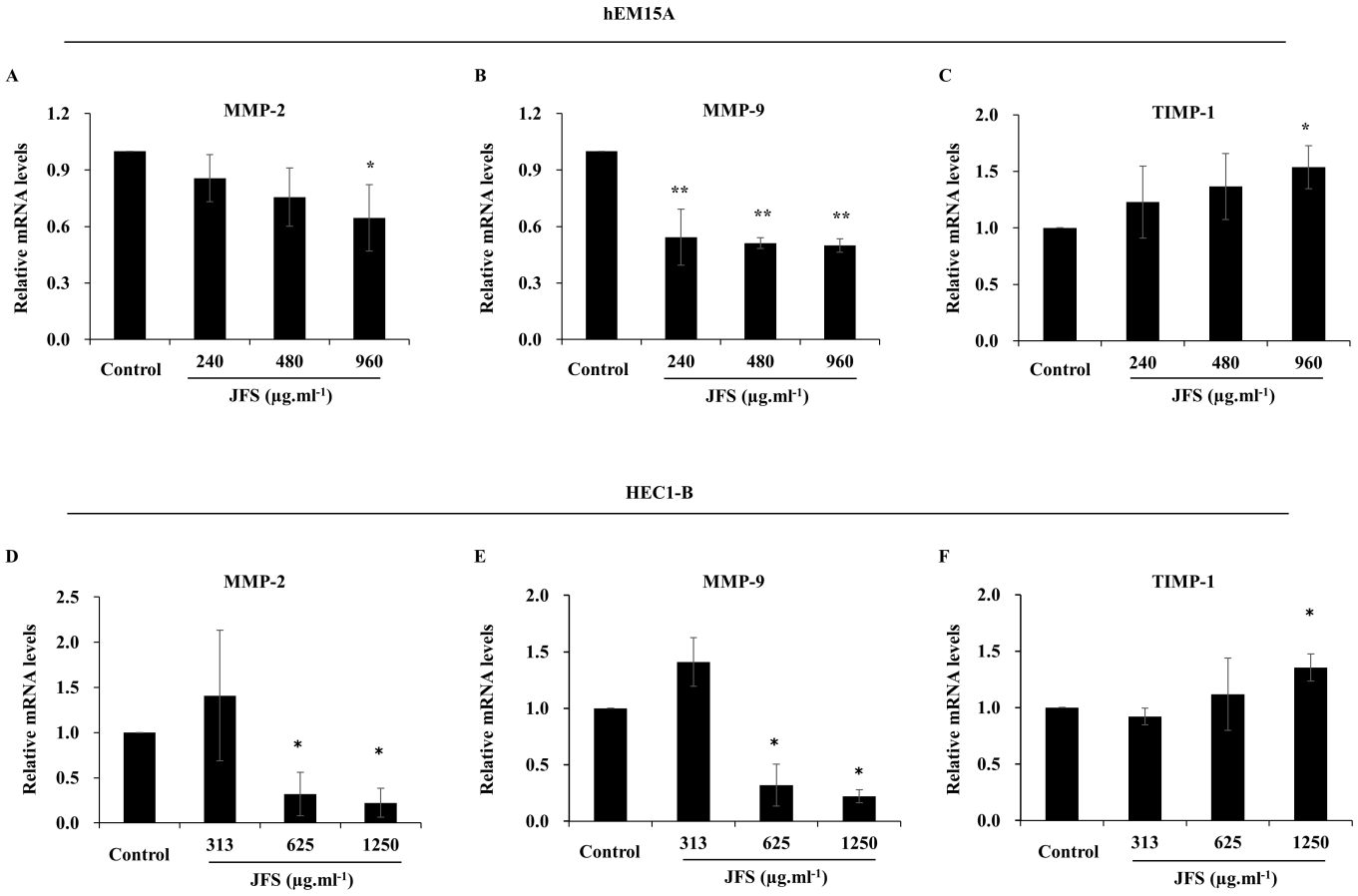

Figure 4

Gene expression of MMP/TIMP signaling adjusted by JFS. The mRNA levels of MMP-2, MMP-9, and TIMP-1 were detected by qPCR in hEM15A (A–C) and HEC1-B (D–F) cells. *P<0.05 to control group, **P<0.01 to control group. Columns, mean (n=3). Bars, SD. JFS, Jiawei Foshou San.

Figure 5

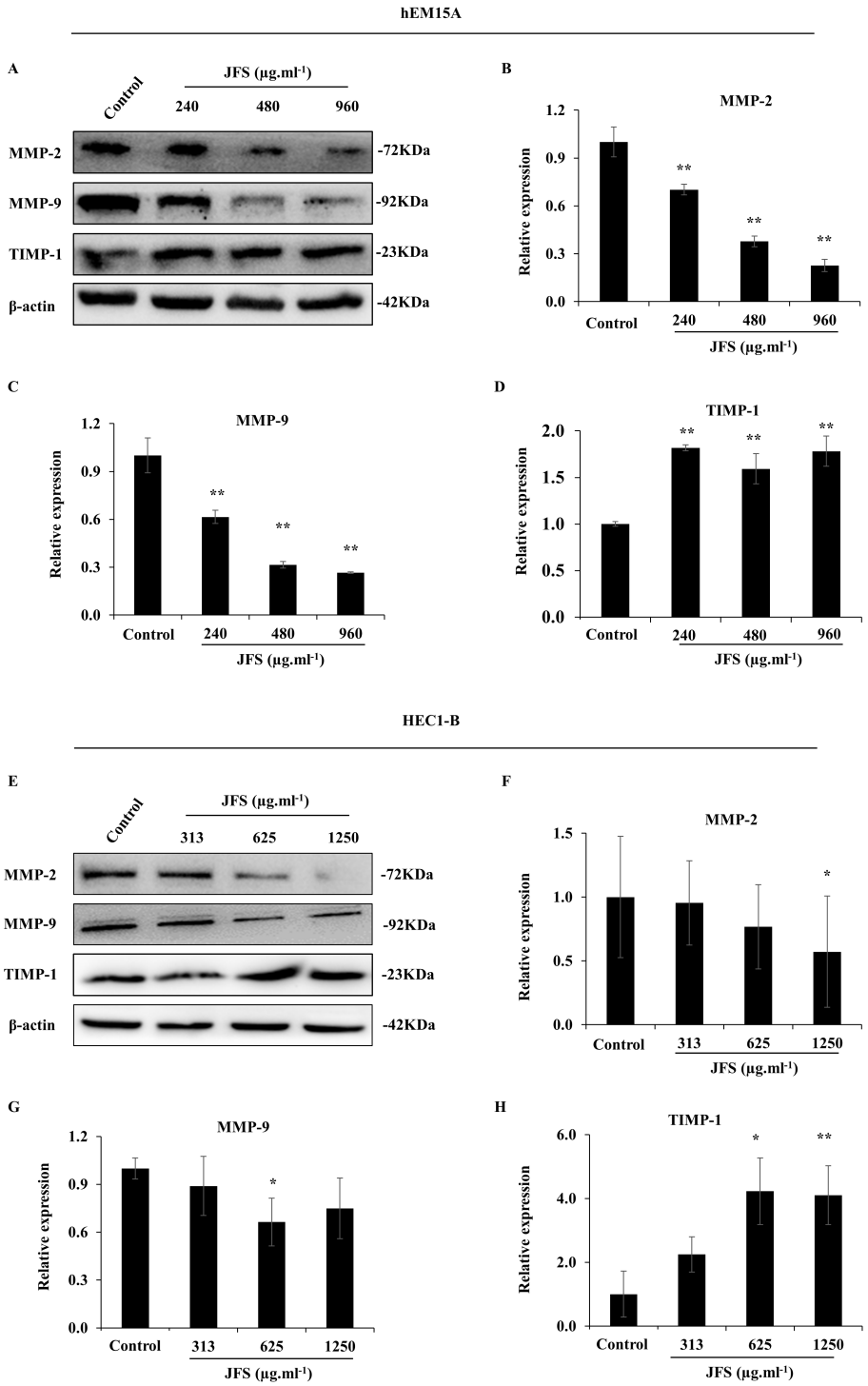

Figure 5

Modification of MMP/TIMP signaling protein treating with JFS. The protein levels of MMP-2, MMP-9, and TIMP-1 were detected by western blot in hEM15A (A–D) and HEC1-B (E–H) cells. The ratio of MMP-2, MMP-9, and TIMP-1 with β-actin were shown. *P<0.05 to control group, **P<0.01 to control group. Columns, mean (n=3). Bars, SD. JFS, Jiawei Foshou San.

Figure 6

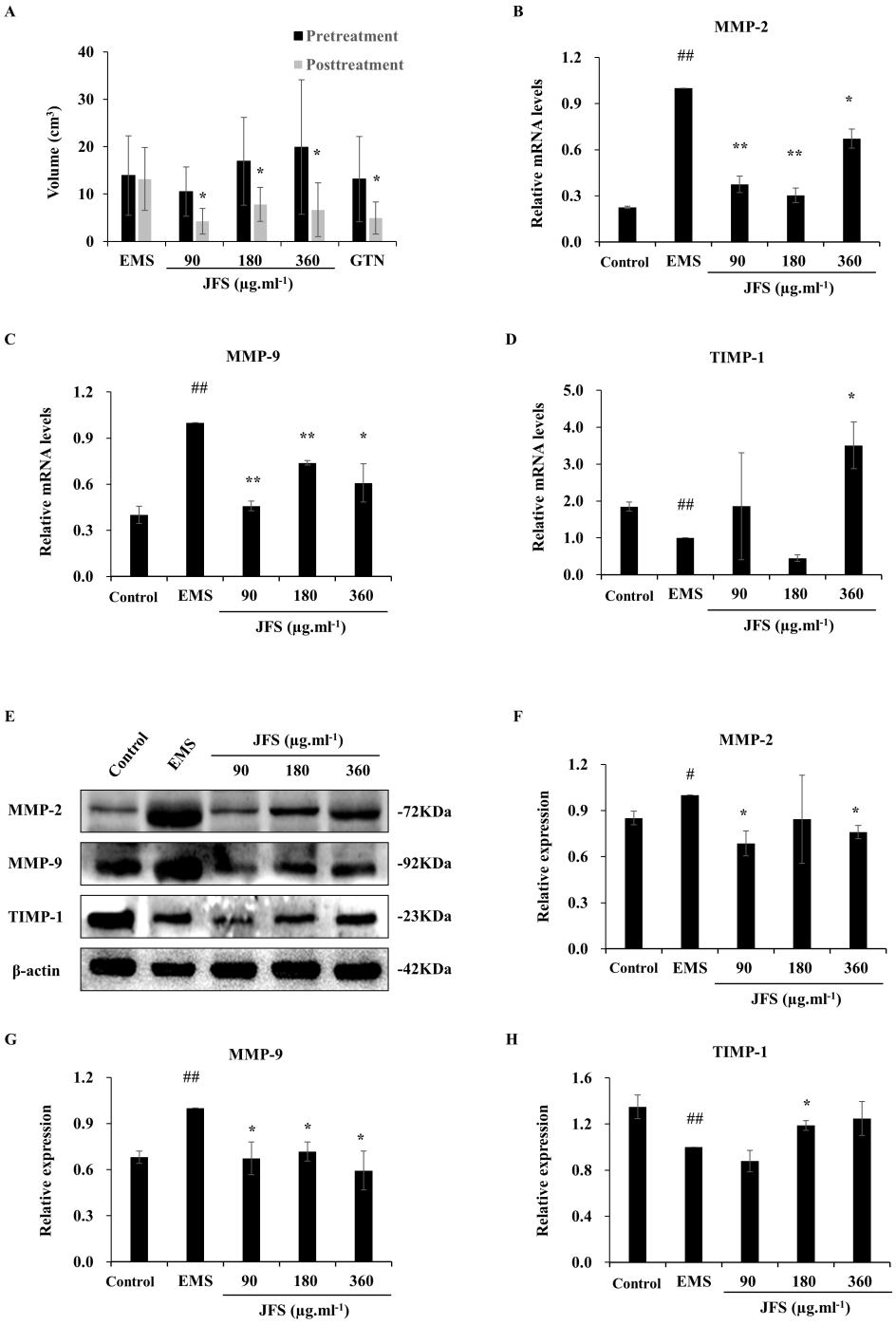

Figure 6

Regulation of JFS on xenograft endometriosis. (A) The volume of ectopic endometrium was detected by vernier caliper in xenograft endometriosis model. ∗P< 0.05 to pretreatment. Columns, mean (n = 6). (B–D) The mRNA levels of MMP-2, MMP-9, and TIMP-1 were detected by qPCR in different groups. (E–H) The protein levels of MMP-2, MMP-9, and TIMP-1 were measured by western blotting, and the ratio of MMP-2, MMP-9, and TIMP-1 with β-actin were shown. # P< 0.05 to control, ## P< 0.01 to control, ∗ P< 0.05 to

EMS, ∗∗ P< 0.01 to EMS. Columns, mean (n = 3). Bars, SD. EMS, endometriosis; JFS, Jiawei Foshou San; GTN, gestrinone.